ANALYSIS OF LIQUID METAL MHD FLUID FLOW AND HEAT TRANSFER USING THE KAT CODE

T. Kunugi*, M. S. Tillack, and M. A. Abdou
6288 Boelter Hall
Mechanical, Aerospace, and Nuclear Engineering Department
University of California, Los Angeles, CA90024
(213)825-5099

ABSTRACT

A new computer code has been developed with the capability to model laminar liquid metal fluid flow and heat transfer in relatively complex geometries at parameter values greater than previously possible with a transient 3-D "full" numerical solution of the MHD equations. The full solution method, which includes viscous and inertial terms, provides an exact solution for boundary layers and is valid over a wide range of flow parameters. Previous attempts at numerically solving the full MHD equations have been limited in the range of magnetic field strengths (B) and Reynolds number (Re) which could be accurately modelled. Numerical techniques for treating problems at high B and Re are implemented in this code, named KAT.

The KAT code is written in rectangular coordinates. with a sophisticated mesh generator and boundary condition input routines. Single-duct and multiple-duct geometries can be modelled with arbitrary wall conductivity and magnetic field variation throughout the solution domain. The code has been tested and benchmarked against analytical solutions and fully-developed very highly accurate numerical solution obtained by 2-D finite element method (FEM). The KAT solutions are in very good agreement with analytic and FEM solutions. The KAT code was applied to a right-angle rectangular bend problem with inclined B-field. Finally, the capabilities of the code and future applications are discussed.

INTRODUCTION

Conditions present in a high-field tokamak reactor often allow relatively accurate solutions for MHD fluid flow using the so-called "core flow approximation," in which inertia and viscous terms are omitted or treated in a simplified way.[1] The core flow approximation allows a much simpler numerical solution as compared to solving the full Navier-Stokes equation.

However, there are several reasons why a full 3-D solution capability for the MHD equations is highly desirable:

1. The full solution is very general.
- no fundamental approximations are made, so corrections are not required (e.g., for side layers)
- more geometric capability exists (compared to the "reduced" core solution). For example, the KAT code treats completely arbitrary 3-D magnetic field distribution and any geometry which can be framed in rectangular coordinates.
- the code can be extended in a straightforward way for unsteady, finite magnetic Reynolds number (Re_m), turbulence modelling, etc.

2. The full solution has a wider potential range of applicability, particularly at lower parameter ranges where the core solution breaks down.

3. Some specific geometries are expected to exhibit inertial effects, which cannot be treated with a core solution. E.g.,
- abrupt changes in geometry (orifice, manifold)
- moderate changes in high-velocity layers (side layers)
- flow situations with large parallel component of B

4. Some issues depend more strongly on boundary layers, particularly heat and mass transport. For developing flow, boundary layers are more accurately treated by a full solution.

The primary drawback to the full solution is the large amount of computer memory and time needed to solve very complex problems. In this regard, advanced numerical methods can help to make the full solution more tractable for a wide array of geometries of interest for fusion.

Previous attempts at full solutions have met with limited success.[2-4] Accuracy and/or convergence were poor and geometric capability limited.

The KAT code has been developed with the goal of treating generalized Cartesian geometries at parameter ranges approaching or exceeding Ha=1000, Re=1000, N=1000. This includes single-duct (straight ducts, various bends, orifices) and multiple-duct geometries (parallel channels, manifolds).

* permanent address:
Japan Atomic Energy Research Institute,
801-1 Mukouyama, Naka-Machi, Naka-Gun, Ibaraki-Ken, 311-02, Japan

The code has been tested by comparing with analytic and highly accurate 2-D FEM solutions.[5] Parameter ranges as high as N=200, Re=500, and Ha=316 have shown excellent agreement. Moreover, in order to show the potential of the KAT code for more complex geometry, the code was applied to a right-angle rectangular bend problem with inclined B-field. Future directions for the KAT code and the full solution in general are discussed in the conclusions.

BASIC EQUATIONS

The governing equations are written in non-dimensional form, including continuity, the momentum equation, the energy equation, and the electric potential equation (derived from the divergence of Ohm's law):

$$\nabla^* \cdot \mathbf{u}^* = 0 \tag{1}$$

$$\frac{\partial \mathbf{u}^*}{\partial t^*} + (\mathbf{u}^* \cdot \nabla^*)\mathbf{u}^* = -\nabla^* p^* + N(\mathbf{J}^* \times \mathbf{B}^*) + \frac{1}{Re}\nabla^{*2}\mathbf{u}^* - \frac{Gr}{Re^2}\theta \tag{2}$$

$$\frac{\partial \theta}{\partial t^*} + (\mathbf{u}^* \cdot \nabla^*)\theta = \frac{1}{Pe}\nabla^{*2}\theta + Ec\left(N\frac{J^{*2}}{\sigma^*} + Q^*\right) \tag{3}$$

$$\nabla^* \cdot (\sigma^* \nabla^* \phi^*) - \nabla^* \cdot (\mathbf{u}^* \times \mathbf{B}^*) = 0 \tag{4}$$

The variables are normalized as shown in Table 1.

Table 1. Non-dimensional parameters

$x^* = \frac{x}{L_o}$	$\sigma^* = \frac{\sigma}{\sigma_f}$
$u^* = \frac{u}{u_o}$	$Re = \frac{u_o L_o}{\nu}$
$B^* = \frac{B}{B_o}$	$Pe = Re\ Pr$
$J^* = \frac{J}{\sigma_f u_o B_o}$	$N = \frac{Ha^2}{Re} = \frac{\sigma_f B_o^2 L_o}{\rho u_o}$
$\phi^* = \frac{\phi}{u_o L_o B_o}$	$Ha^2 = \frac{\sigma_f B_o^2 L_o^2}{\mu}$
$p^* = \frac{p}{\rho u_o^2}$	$Gr = \frac{\beta g L_o^3 (T_1 - T_o)}{\nu^2}$
$t^* = \frac{t}{L_o/u_o}$	$Ec = \frac{u_o^2}{c_p(T_1 - T_o)}$
$Q^* = \frac{Q L_o}{\rho u_o^3}$	$\theta = \frac{T - T_o}{T_1 - T_o}$

where Re is Reynolds number, Pe is Peclet number, Gr is Grashof number, Ec is Eckert number, Ha is Hartmann number and N is the interaction parameter. Q is volumetric heat source. σ_f is electrical conductivity of fluid. T is temperature. T_o and T_1 are reference temperatures.

SOLUTION ALGORITHM

The solution procedure uses primitive variables (u, v, w, p, ϕ, θ). A time-advancing technique is applied, in which a steady-state problem is treated by solving a time-dependent problem with the initial guess serving as the initial condition. Equations are discretized by a finite difference (finite control volume) method on the well-known staggered-grid system.

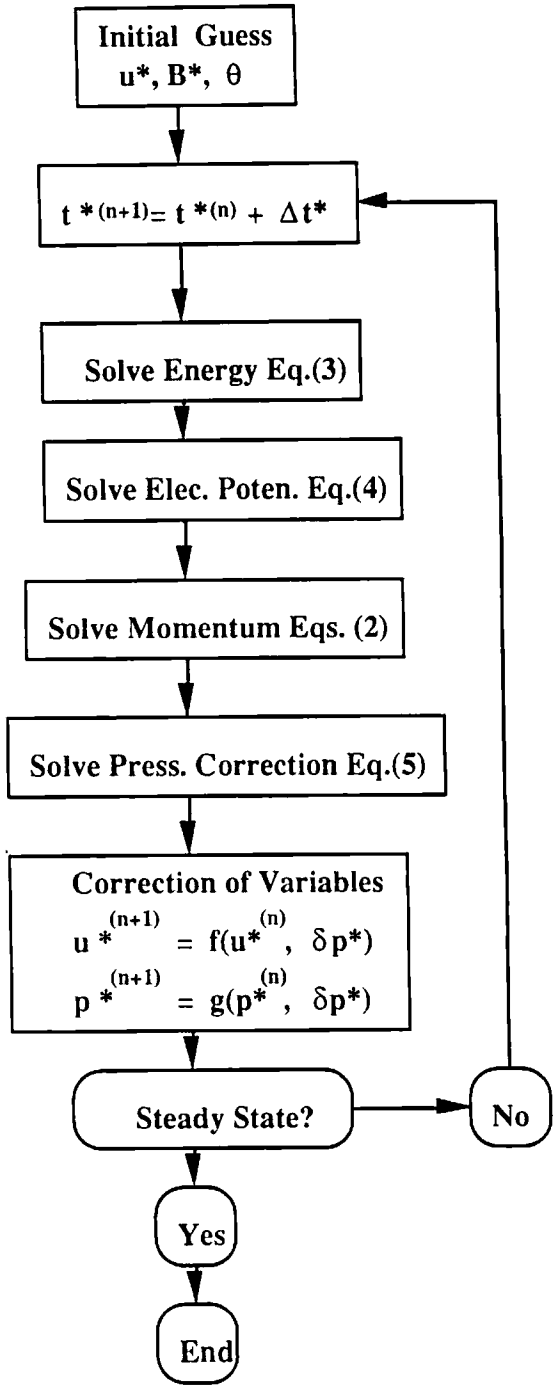

Figure 1. Flow Chart for KAT

The non-linear convective terms are treated by the CONDIF method (Controlled Numerical Diffusion with Internal Feedback).[6] This scheme is based on the central-differencing scheme without anomalous numerical oscillation and can achieve good convergence and high accuracy at relatively high cell Reynolds number.

The pressure correction method is critical to obtaining good convergence in MHD problems. In KAT, the coupling between pressure and velocity fields is obtained by solving the pressure correction equation:

$$\nabla^{*2}\delta p^{*} = \frac{\nabla^{*}\cdot\tilde{u}^{*}}{\Delta t^{*}} \qquad (5)$$

where, $\delta p^{*} = p^{*(n+1)} - p^{*(n)}$ (here, n is time step index), Δt^{*} is time increment and $\nabla^{*}\cdot\tilde{u}^{*}$ is the residual of mass.

The flow chart for KAT code is shown in Figure 1. Following the initial velocity($\mathbf{u}^{*}$), magnetic field($\mathbf{B}^{*}$) and temperature(θ) guess, at first, the energy equation is solved and the electric potentials(ϕ^{*}) are solved using the potential equation. Electric current($\mathbf{J}^{*}$) is obtained from Ohm's law using $\mathbf{u}^{*}$, $\mathbf{B}^{*}$ and ϕ^{*}, and substituted into the momentum equation in order to evaluate the Lorentz force term($\mathbf{J}^{*}\times\mathbf{B}^{*}$). At this point, the momentum equation is solved for a tentative velocity($\tilde{\mathbf{u}}^{*}$). The pressure correction equation is then solved to get the amount of the pressure correction (δp^{*}). Finally, all variables of the velocity and pressure fields are corrected. Functions used in the correction process of variables, f and g, are defined as follows:

$$f(\mathbf{u}^{*(n)}, \delta p^{*}) = \mathbf{u}^{*(n)} - \Delta t^{*}\nabla^{*}\delta p^{*},$$
$$g(p^{*(n)}, \delta p^{*}) = p^{*(n)} + \delta p^{*}. \qquad (6)$$

This correction provides the solution at the end of a given time step. Until steady-state is achieved, this entire procedure is repeated.

In the KAT code, two Poisson equations, eqs. (4) and (5), are solved iteratively in each time step. These computations are very time consuming processes, especially at the beginning of computation. In order to reduce the computational time, a cyclic reduction successive over relaxation method(CRSOR) is used as the matrix solver. This method is suitable for vector machines such as CRAY computers.

BENCHMARKING

Initial tests of KAT were performed in straight rectangular channels with insulated and conducting walls and constant magnetic field. Slug flow inlet conditions were applied. The velocities were developing in the downstream direction and achieved a fully-developed profile within the solution domain. This fully-developed solution was then compared with analytic and 2-D FEM solutions to test the accuracy.

Figure 2 shows the problem definition and geometry.

The channel width was "2a" and the channel length was "4a", here "a" was the channel half-width. The boundary conditions include zero velocity at the wall, so-called "non-slip velocity condition", and zero current out of the channel. At the outlet, a constant pressure(p^{*}=0.0) was specified. The parameters of this MHD flows were in the ranges of Ha=100~316, N=200 and Re=50~500.

In the case of conducting walls, the wall conductance ratio, c, was 0.01.

$$c = \frac{\sigma_w\, t}{\sigma_f\, a} \qquad (7)$$

where t is the wall thickness, and σ_w and σ_f are the wall and fluid conductivities.

The computations were carried out only for a half-domain of the channel in z-direction due to symmetry. A typical number of grids was 16000[(x,y,z)=(20,40,20)]. The CPU time was around 2 hours per case.

For the insulated channel case, the velocity prediction of KAT in the fully-developed region is compared with the 2-D FEM solution of MH2D[6] in Figure 3. Agreement is very good. MH2D was tested against Shercliff's analytic solution[7] with perfect agreement.

Figure 4 shows the velocity profile in the Hartmann layer. The result of KAT is in excellent agreement with the classical Hartmann profile.

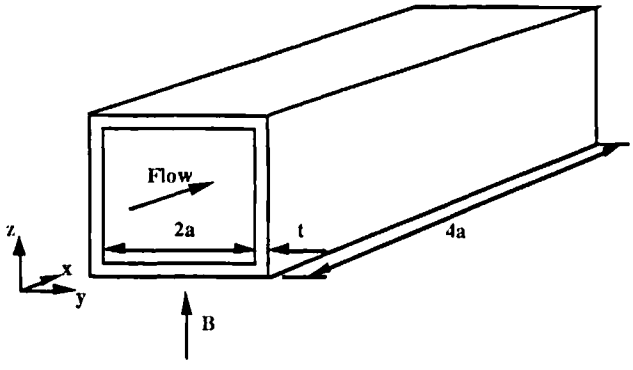

Figure 2. Problem definition and geometry of the channel for the developing flow test cases.

For the conducting channel case, the velocity profile in the side layer is compared with the prediction of MH2D in Figure 5. Again, very good agreement is found in the fully-developed regime.

Figure 6 shows the tendency of the solution behavior as Ha increases from 100 to 316 (i.e., Re increases from 50 to 500 at fixed N). The core velocity decreases as Ha increases, while on the other hand, the side layer velocity increases as Ha increases.

A 3-D view of the velocity profile at the fully-developed flow region, in case of Ha=200 and c=0.01, is shown in Figure 7. The velocity profiles in the side layer and Hartmann layer are clearly visible.

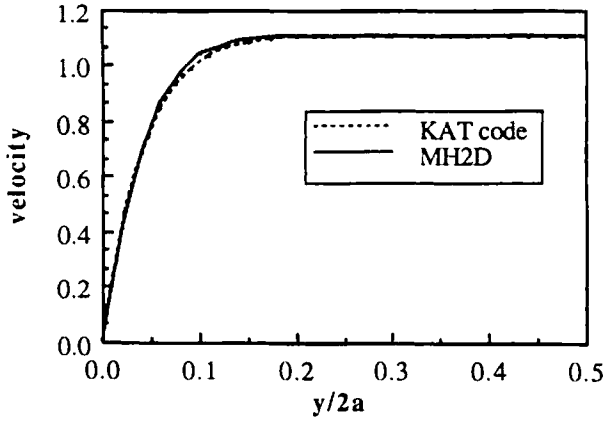

Figure 3. Side layer velocity(u) profile at the centerline – comparison between KAT and MH2D in the fully-developed flow region.

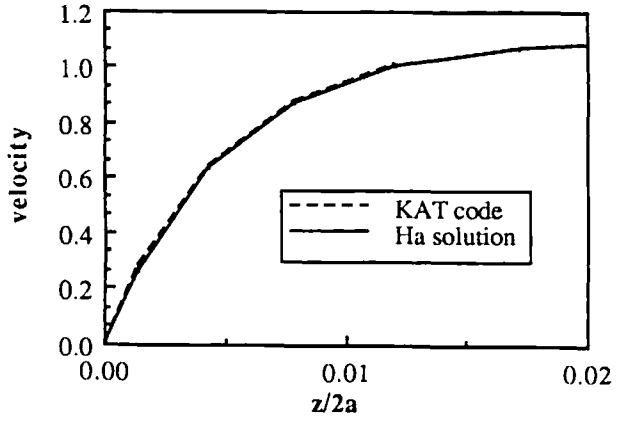

Figure 4. Hartmann layer velocity(u) profile at the centerline – comparison between KAT and Hartmann's solution in the fully-developed region.

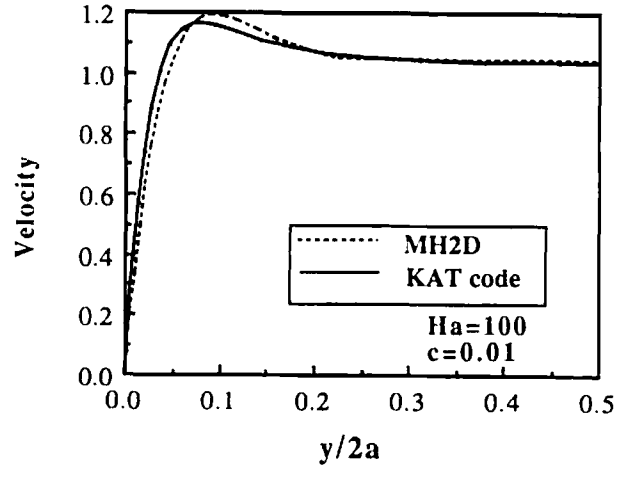

Figure 5. Comparison of side layer velocity(u) profile with MH2D in the fully-developed region

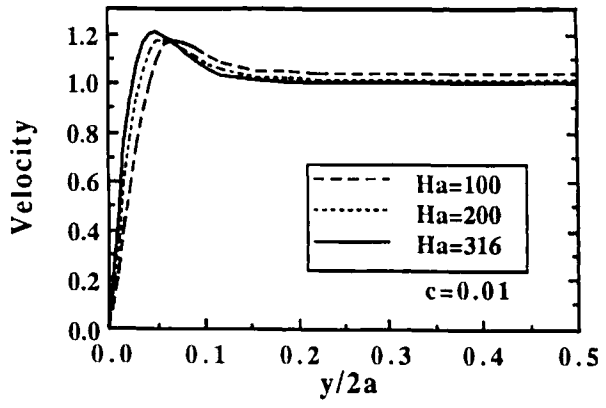

Figure 6 Side layer velocity profiles under various Ha.

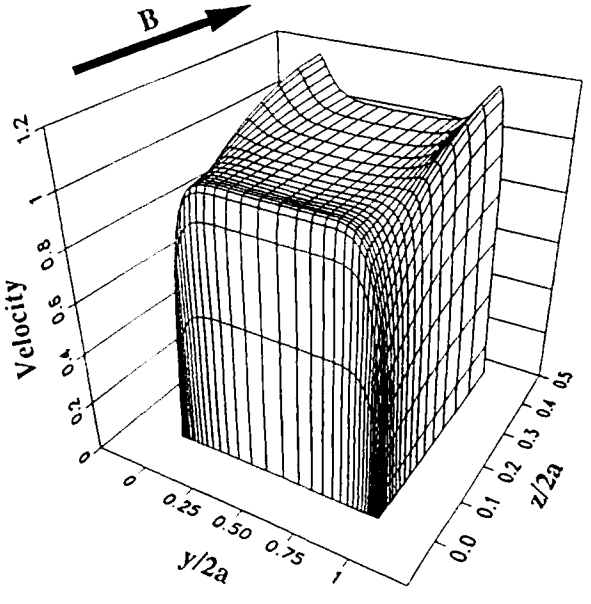

Figure 7 3-D view of the velocity profile at the fully-developed flow region in case of Ha=200 and c=0.01.

NUMERICAL ANALYSIS OF A RIGHT-ANGLE RECTANGULAR BEND

In the previous section, the accuracy of the KAT code was discussed. In this section, the potential of the KAT code is discussed through the application to a problem with more complicated geometry and boundary conditions.

In order to show the potential of the KAT code, a right-angle rectangular bend problem was analyzed. The problem definition and geometry are shown in Figure 8. The channel cross-section was a square shape, and its width was "2a". The length of the channel both before and after the bend part were "4a". A constant inclined

magnetic field $B^*=(B_x^*,B_y^*,B_z^*)$ was applied: i.e., $B_x^*=\cos 45^o$, $B_y^*=\sin 45^o$ and $B_z^*=0$. The boundary conditions included non-slip velocity at the wall, and zero current out of the channel. At the outlet, a constant pressure ($p^*=0.0$) was specified.

The grid configuration in the x-y plane is shown in Figure 9. The number of grids was 44x44x16, and CRAY-I CPU time was around 5 hours for this case. The grid lines were concentrated near all the boundaries.

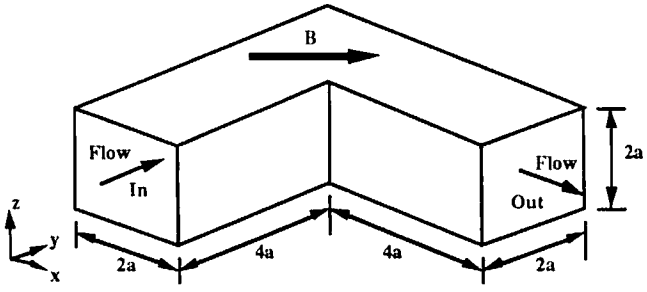

Figure 8 Problem definition of the right-angle rectangular bend flow. Parameters are Ha=100 (Re=50) and c=0.01.

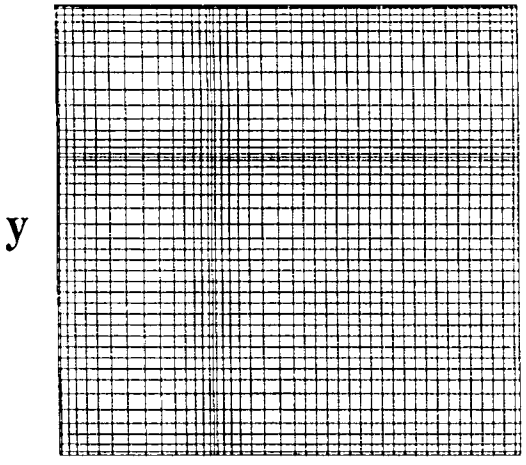

Figure 9 Grid configuration on the x-y plane.

Figures 10-(a),(b) show the velocity vector fields on the x-y plane at near the wall(a) and center(b). Near the wall, no stagnation and separation/recirculation region appears. However, at the center plane, a large separation/recirculation region is formed at the corner of the bend. Small separation is observed near the outlet due to the specified pressure boundary condition. This kind of vortex would disappear if the length of the channel after

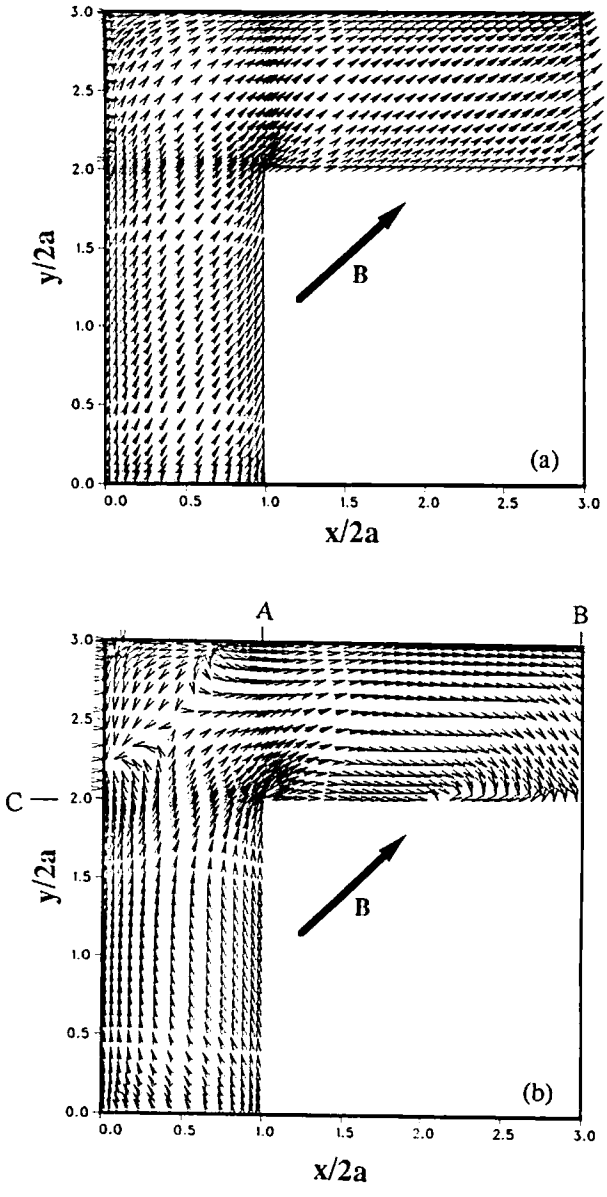

Figure 10 Velocity vector field on the x-y plane. (a) near the wall, (b) at the center plane.

the bend was much longer, but a longer channel calculation would need much longer computational time.

Figure 11 shows the velocity profiles at the corner and outlet (see the marks A, B, and C in Fig.10). Line A is near the corner and line B is near the outlet.. It is found that the peak velocity position moves from inner wall side(y/2a~2) to outer wall side(y/2a~3). This is due to the inclined magnetic field. The symmetric feature of this flow around the corner is shown in Figure 12. This figure shows that the two velocity components normal to the the corner, u and v, have the same magnitude and profile [the u-profile is shown at A, and the v-profile is shown at C in Fig.10].

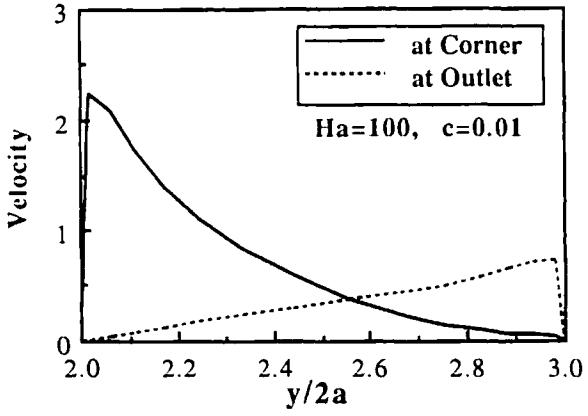

Figure 11 Velocity profiles at the corner along line A and at the outlet along line B in Fig. 10.

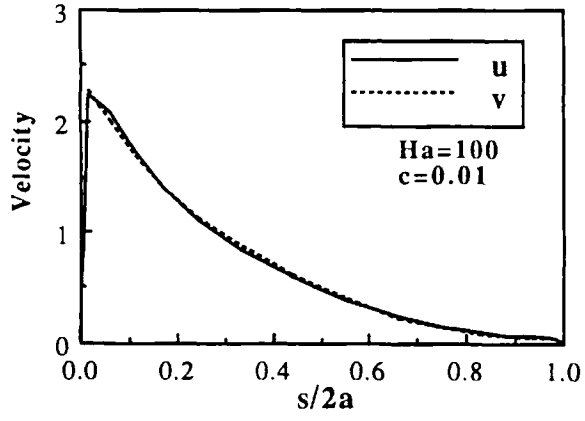

Figure 12 Symmetric feature of the flow around the corner, where, s is the normal distance from the corner. [the u-profile is shown at A, and the v-profile is shown at C in Fig.10.]

CONCLUSIONS

A new computer code has been developed with the capability to model laminar liquid metal fluid flow and heat transfer in relatively complex geometries at parameter values greater than previously possible with a transient 3-D "full" numerical solution of the MHD equations.

This KAT code has the potential to solve many MHD fluid flow and heat transfer problems. In the near future, the KAT code will be applied to more difficult problems which include more complicated geometries and boundary conditions. For the fusion reactor applications such as liquid metal cooling blanket design, it is difficult to analyze the whole blanket module because the present existing computer has some limitation such as CPU time and the memory space. However, it could be analyzed for the individual section or component such as manifold and orifice, etc.

In order to obtain the solutions with less CPU time, the matrix solver will have to be improved. And also, vectorization of more than 98% of the code should be possible. For the fusion reactor relevant conditions such as $Ha=10^3 \sim 10^5$ and full blanket, it will need an advanced computer which has very high-speed computational ability and very big main memory space around 100 times more than the existing computer system.

ACKNOWLEDGEMENTS

This work was jointly supported by Japan Atomic Energy Research Institute and the U.S. Department of Energy under grant #DE-FG03-86ER52123.

REFERENCES

1. M. S. TILLACK, "Application of the Core Flow Approach to MHD Fluid Flow in Geometric Elements of a Fusion Reactor Blanket," Liquid Metal Magneto-hydrodynamics, J. Lielpeteris and R. Moreau editors, Kluwer Academic Publishers, Dordrecht (1989).

2. C. N. KIM and M. A. ABDOU, "Numerical Method for Fluid Flow and Heat Transfer in Magneto-hydrodynamic Flow," Fusion Technology 15(2), Part 2, March (1989).

3. B. SINGH and J. LAL, "Effect of Magnetic Field Orientation and Wall Conductivity on MHD Channel Flows Using Finite Element Method," Comp. Meth. in App. Mech. and Eng. 40, 159-170 (1983)

4. N. S. WINOWICH and W. F. HUGHES, "A Finite-Element Analysis of Two-Dimensional MHD Flow," Liquid Metal Flows and Magnetohydrodynamics, ed. by H. Branover, P. S. Lykoudis, and A. Yakhot, pp. 313–322 (1983).

5. M. S. TILLACK, A. Y. YING, and H. HASHIZUME, "The Effect of Magnetic Field Alignment on Heat Transfer in Liquid Metal Blanket Channels," Proceedings of 13th Symposium on Fusion Engineering, Knoxville TN, October (1989).

6. A. K. RUNCHAL, "CONDIF: A Modified Central-Differencing Scheme with Unconditional Stability and Very Low Numerical Diffusion," Int. Heat Transfer Conf., 404–408 (1986)

7. J. A. SHERCLIFF, "Steady Motion of Conducting Fluids in Pipes Under Transverse Magnetic Fields," Proc. Cambridge Phil. Soc. 49(1) 136-144, 1953.